

Protein Folding Drives Disulfide Formation

Pallav Kosuri,^{1,2,*} Jorge Alegre-Cebollada,² Jason Feng,² Anna Kaplan,² Alvaro Inglés-Prieto,⁵ Carmen L. Badilla,² Brent R. Stockwell,^{2,3,4} Jose M. Sanchez-Ruiz,⁵ Arne Holmgren,⁶ and Julio M. Fernández^{2,*}

¹Graduate Program in Biochemistry & Molecular Biophysics

²Department of Biological Sciences

³Department of Chemistry

⁴Howard Hughes Medical Institute

Columbia University, New York, NY 10027, USA

⁵Facultad de Ciencias, Departamento de Química-Física, Universidad de Granada, 18071 Granada, Spain

⁶Medical Nobel Institute for Biochemistry, Department of Medical Biochemistry and Biophysics, Karolinska Institutet, 17177 Stockholm, Sweden

*Correspondence: pallav@caa.columbia.edu (P.K.), jfernandez@columbia.edu (J.M.F.)

<http://dx.doi.org/10.1016/j.cell.2012.09.036>

SUMMARY

PDI catalyzes the oxidative folding of disulfide-containing proteins. However, the sequence of reactions leading to a natively folded and oxidized protein remains unknown. Here we demonstrate a technique that enables independent measurements of disulfide formation and protein folding. We find that non-native disulfides are formed early in the folding pathway and can trigger misfolding. In contrast, a PDI domain favors native disulfides by catalyzing oxidation at a late stage of folding. We propose a model for cotranslational oxidative folding wherein PDI acts as a placeholder that is relieved by the pairing of cysteines caused by substrate folding. This general mechanism can explain how PDI catalyzes oxidative folding in a variety of structurally unrelated substrates.

INTRODUCTION

Protein folding is a sensitive reaction that can be easily affected by a multitude of factors such as mutations and changes in the physical or chemical environment. Failure to correctly fold is the basis of numerous disorders of central importance to modern medicine (Dobson, 2003). In particular, the third of human proteins that traverse the secretory pathway and that possess disulfide bonds pose unresolved challenges to our understanding of protein folding and disease (Gething and Sambrook, 1992; Ron and Walter, 2007; Schröder and Kaufman, 2005). Protein disulfide isomerase (PDI) introduces disulfide bonds into folding proteins and is the main catalyst of oxidative folding in humans (Wilkinson and Gilbert, 2004). Recent studies have revealed a link between disulfide chemistry and the pathogenesis of misfolding diseases and specifically implicated PDI as a novel target for treatment of several neurodegenerative disorders including Alzheimer's disease (Hoffstrom et al., 2010; Uehara et al., 2006). These studies stress the importance of understanding how PDI catalyzes oxidative folding.

Human PDI catalyzes the formation of disulfides (oxidase activity) as well as the rearrangement of incorrectly formed disulfide bonds (isomerase activity) (Wilkinson and Gilbert, 2004). The enzyme consists of two catalytically active A domains and two redox-inactive B domains. Isolated A domains have been shown to effectively catalyze the introduction of disulfides into protein substrates; meanwhile the full-length protein is generally thought to be required for efficient isomerase activity (Darby and Creighton, 1995b). PDI belongs to a ubiquitous family of enzymes that catalyze thiol-disulfide exchange (Wilkinson and Gilbert, 2004). In addition to PDI, this family includes other oxidoreductases such as thioredoxin (TRX), glutaredoxin, and the bacterial Dsb enzymes (Martin, 1995). All of these enzymes share a characteristic structural fold and a highly conserved Cys-X-X-Cys motif in their active sites (Martin, 1995). Their mechanism of action has been revealed through numerous studies over the past 40 years. In all cases, the reaction mechanism involves the formation of a mixed disulfide between a cysteine in the substrate and the N-terminal cysteine in the active site of the enzyme (Holmgren, 1985; Walker et al., 1996) (Figure S1 available online). The C-terminal cysteine can attack and cleave the mixed disulfide, thereby spontaneously releasing the enzyme (Walker and Gilbert, 1997; Wilkinson and Gilbert, 2004). Whereas spontaneous release is necessary during reduction of substrate disulfide bonds, it is unknown how this activity affects catalysis of oxidative folding.

Secretory proteins are synthesized as linear polypeptides and emerge from the ribosomal channel via the translocon into the endoplasmic reticulum (ER) (Rapoport et al., 1996; Van den Berg et al., 2004; Walter et al., 1984). Emerging sequentially into the ER, the nascent polypeptide encounters PDI, which catalyzes cotranslational oxidative folding (Bulleid and Freedman, 1988; Molinari and Helenius, 1999). This reaction is mediated by the formation of a mixed disulfide bond between the PDI enzyme and a cysteine in the nascent polypeptide (Figure 1A) (Frang and Kaiser, 1999; Gilbert, 1995; Sevier and Kaiser, 2002). The mixed disulfide is then transferred to the folding polypeptide. Given the crucial roles of mixed disulfides in oxidoreductase catalysis, many studies have been focused on these ephemeral intermediates. The molecular structures of mixed disulfide complexes have been reported for several enzymes

(Dong et al., 2009; Paxman et al., 2009; Qin et al., 1995). In addition, mixed disulfide complexes in the process of oxidative folding have been characterized in living cells (Di Jeso et al., 2005; Kadokura and Beckwith, 2009; Kadokura et al., 2004; Molinari and Helenius, 1999). Although these studies have provided us with snapshots of mixed disulfide complexes, their dynamics during oxidative protein folding remain unknown. In order to study the intersection of covalent chemistry and protein folding, a method is needed that can independently measure these two concurrent processes.

Here we demonstrate single-molecule techniques that measure the kinetics of enzyme attachment and release and the kinetics of protein oxidation and folding. We used an atomic force microscope (AFM) to mimic the initial stages of oxidative folding by extending an individual polypeptide to a state wherein the substrate cysteines were spatially separated, and a mixed disulfide complex was formed with the catalytic domain A1 from human PDI (hereafter referred to as PDIA, Figure 1B). We then allowed the polypeptide to refold in the absence of external force and probed the progress of oxidative folding by applying additional force pulses. Our data are consistent with a model in which PDIA acts as a placeholder that allows the substrate to guide the pairing of cysteines into native disulfide bonds. This mechanism is general in its nature and therefore does not require substrate specificity.

RESULTS

Creating a Mixed Disulfide Complex between PDIA and a Single Unfolded Protein

Formation of a PDI-substrate mixed disulfide is thought to enable oxidative folding of newly synthesized proteins. We sought to create such a mixed disulfide complex and, starting from this state, study the progression of oxidative folding. A mixed disulfide complex can be formed through two pathways (Figure S1). In the first pathway, an oxidized PDI enzyme reacts with a free substrate cysteine (Frand and Kaiser, 1999; Tu et al., 2000). In the second pathway, the mixed disulfide is formed when reduced PDI reacts with a substrate disulfide (Lundström and Holmgren, 1990). Regardless of the pathway, the resulting mixed disulfide complex is identical. Although we could use both pathways (see Figures 6 and S7), the second pathway proved more advantageous in our experiments because we could then directly detect the formation of the mixed disulfide, as described in detail below.

We used in our experiments human PDI A1 (PDIA). Although essentially inactive in disulfide isomerization as compared to the full-length enzyme, PDIA is sufficient for catalysis of oxidative folding (Darby and Creighton, 1995b). The substrate we chose was the 27th Ig domain from human cardiac titin containing a buried disulfide between residues 32 and 75 (hereafter referred to as I27³²⁻⁷⁵), which has been well characterized in the past (Ainavarapu et al., 2007; Wiita et al., 2006, 2007).

Our strategy to establish mixed disulfide complexes is illustrated in Figure 1C, and an experimental recording is displayed in Figure 1D. We used a custom-built AFM to apply a constant calibrated force to the termini of a single I27³²⁻⁷⁵ protein, while measuring its extension (Fernandez and Li, 2004). A force of

130–150 pN enables protein unfolding but does not break any of its covalent bonds (Grandbois et al., 1999; Wiita et al., 2006). The polypeptide chain can thus unravel only up to the disulfide bond, resulting in the 11 nm extension step seen in the recording (Figure 1D). Meanwhile, the 11 nm extension exposes the 32–75 disulfide to the solvent and enables reactions with enzymes present in the surrounding media (Wiita et al., 2006). In Figure 1D, a reduced PDIA enzyme present in solution reacts with the now solvent-exposed disulfide, creating a mixed disulfide. The enzymatic reaction is captured as a 14 nm step that results from mechanical unraveling of the rest of the substrate as soon as the original disulfide is broken. A 14 nm step in our experiments thus indicates the formation of a mixed disulfide complex. Once a mixed disulfide was acquired in a fully extended polypeptide, we could proceed to study its effect on protein folding.

Mixed Disulfide Complexes with PDIA Enable Oxidative Folding

We used a three-part experimental protocol consisting of two mechanically equivalent force pulses separated by a refolding interval [*denature* – *folding* – *probe*] to study the effect of PDIA mixed disulfide complexes on the folding of an (I27³²⁻⁷⁵)₈ polypeptide substrate (Figure 1E). A polyprotein was used because it yields multiple events within a single recording, thereby providing a stronger fingerprint of the reactions. Figure 1F shows how each substrate domain was first completely extended and linked to a PDIA enzyme during an initial *denature* pulse, as described in the previous section. The force was subsequently switched off, and the substrate was allowed to fold for a set time $\Delta t_{\text{folding}}$ (Δt_F). In order to detect the formation of disulfide bonds and protein folding during Δt_F , we once again applied force, thereby halting the folding reaction. This *probe* pulse was identical to the initial *denature* pulse and in the same manner allowed us to detect folded domains and disulfide bonds. A 25 nm step appearing during the *probe* pulse reports that a domain had folded but not formed a disulfide during Δt_F . An 11 nm step, on the other hand, indicates that a domain had folded during Δt_F and also acquired a disulfide. Given that PDIA was present in the surrounding media throughout the experiment, 14 nm steps would be seen in the *probe* pulse if newly formed disulfide bonds were again broken. In summary, a 25 nm step provided a signature of a natively folded domain with no disulfide, whereas an 11 nm step (followed by a 14 nm step) indicated a natively folded domain with a disulfide (Figure 1F).

Figure 1G shows an experimental recording of the [*denature* – *folding* – *probe*] experiment in a solution containing reduced PDIA, and Figure 1H shows histograms of the step sizes detected in several such recordings. During the *denature* pulse, 11 and 14 nm steps were seen, indicating formation of mixed disulfide complexes between PDIA and the substrate. When the force was removed ($\Delta t_F = 5$ s), the substrate rapidly collapsed as seen in the experimental trace (Figure 1G). The 11 and 14 nm steps seen in the *probe* pulse unambiguously showed that disulfides had been formed in the substrate during folding. The reaction path for these domains is readily interpreted. When the force was removed, the substrate collapsed and allowed the free cysteine in each domain to attack the mixed

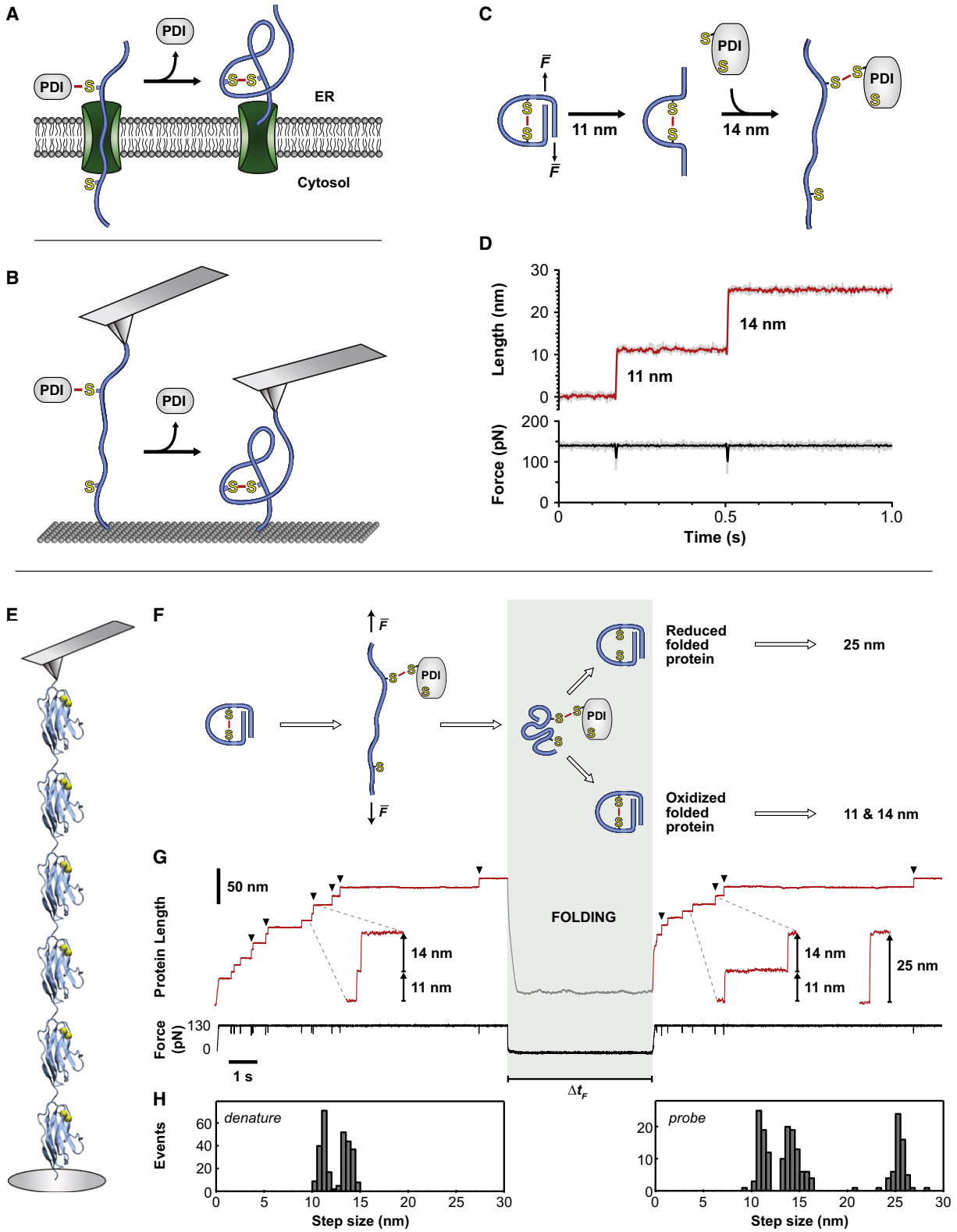


Figure 1. A Single-Molecule Approach to Study Oxidative Folding

(A) As part of the secretory pathway, protein disulfide isomerase (PDI) forms mixed disulfide complexes with nascent polypeptides (blue) undergoing ER translocation. These complexes are thought to enable oxidative folding.

disulfide bond, thus releasing the PDla enzyme and establishing the intramolecular 32–75 disulfide bond. The appearance of 11 nm unfolding steps is consistent with these domains also acquiring their native fold. Additional experiments performed with full-length bovine PDI showed similar results, validating our use of PDla (see Figure S2C for a representative recording).

Detection of Spontaneous Enzyme Release

In addition to 11 and 14 nm steps, 25 nm steps were also seen in the *probe* pulse (Figures 1G, 1H, and S2B), revealing that some substrate domains had folded without forming disulfide bonds. Two scenarios can account for these 25 nm steps: either (1) PDla was still attached to the folded substrate but had failed to introduce the 32–75 disulfide bond, or (2) PDla had spontaneously released before substrate oxidation could be realized. We could thus distinguish between these scenarios by using two oxidoreductase enzymes with vastly different release rates: wild-type (WT) and C35S TRX.

TRX is capable of catalyzing the same reactions as PDI (Carvalho et al., 2006; Debarbieux and Beckwith, 2000; Lundström et al., 1992) but releases spontaneously from the mixed disulfide on a much faster (sub-millisecond) timescale, as inferred from reactions with nonprotein substrates (Chivers and Raines, 1997; Lappi and Ruddock, 2011). Consequently, in a [*denature* – *folding* – *probe*] experiment with WT TRX, all enzymes would have released from the substrate before the end of the *denature* pulse. We would thus expect only 25 nm steps in the *probe* pulse as the substrate folds in the absence of the enzyme. Experiments with TRX confirmed that only 25 nm steps were detected in the *probe* pulse (Figure 2A).

Spontaneous release from the mixed disulfide is mediated by the C-terminal cysteine in the active site of oxidoreductases (Cys35 in TRX). We mutated this cysteine to abolish spontaneous release (TRX C35S, Figure 2B; see also Figure S3). This resulted in the complete absence of 25 nm steps and full oxidation of the substrate (as indicated by 11 and 14 nm steps in the *probe* pulse). Thus, every domain that folded in the presence of a mixed disulfide complex successfully completed oxidative folding. These observations indicate that 25 nm steps are only caused by spontaneous release of the enzyme from the mixed disulfide complex prior to folding, in agreement with scenario (2) described above (see Figure S4C for further support of this

conclusion). We could therefore use 25 nm steps as an indicator of spontaneous enzyme release.

Measurement of the PDla Spontaneous Release Rate

In our experiments, we could detect the formation of individual mixed disulfide complexes (14 nm steps in the *denature* pulse), their presence during protein folding (14 nm steps in the *probe* pulse), and their spontaneous dissociation prior to folding (25 nm steps in the *probe* pulse). By varying the time before folding (the duration of the *denature* pulse, Δt_D ; see Figures 3 and S4A) and measuring the resulting proportion of 25 nm steps in the *probe* pulse, we could thus measure the rate of PDla spontaneous release from a protein substrate. In these experiments, we used a force protocol optimized for long experiments with split *denature* and *probe* pulses (see Experimental Procedures).

For a *denature* pulse duration $\Delta t_D = 5$ s, ~50% of the refolded domains contained disulfide bonds (11 nm, 14 nm steps in *probe* pulse of Figure 3A). In contrast, for $\Delta t_D = 30$ s, the enzymes had more time to release from the mixed disulfide complex, which led to 80% of folded domains not having acquired disulfide bonds (25 nm steps in *probe* pulse of Figure 3B).

Figure 3D shows a simple model of the PDla dissociation process. This model contains three rates, representing the rate of spontaneous enzyme release (k_{off}), the rate of oxidative folding from the mixed disulfide complex (k_{ox}), and the rate of folding of the reduced substrate (k_{fold}). The model also assumes that PDla can dissociate during both Δt_D and Δt_F . Notably, the total amount of refolding remained constant for all values of Δt_D (Figure S4B), leading to the conclusion that k_{ox} and k_{fold} were approximately equal (this is further verified by the kinetic data in Figure 4C). Given that the folding and oxidation rates were similar, it follows that 14 versus 25 nm steps report on the PDla enzyme being “on” and “off,” respectively. We measured the dissociation of PDla as the ratio between the number of 25 nm steps and the total number of refolded domains in the *probe* pulse. In Figure 3C, this dissociated fraction is displayed as a function of total time before probing ($\Delta t_D + \Delta t_F$). We obtained the PDla release rate by fitting these data with a single exponential curve constrained to zero at time zero. The result of the fit was consistent with a spontaneous PDla release rate $k_{off} = 0.10 \pm 0.03$ s⁻¹.

(B) In this study, we used an atomic force microscope (AFM) to create mixed disulfide complexes between PDla enzymes and a single extended protein. Starting from this state, we investigated how PDla catalyzes oxidative folding.

(C) Mixed disulfide complexes were formed by applying a constant stretching force to a folded protein containing a buried disulfide, thus unfolding the protein and exposing the disulfide. A reduced PDla enzyme could then form a mixed disulfide with one of the cysteines in the substrate through S_N2-attack by the enzyme thiolate on the substrate disulfide (charges have been omitted for clarity; see also Figure S1).

(D) In an experimental recording of the end-to-end length of the I27^{32–75} substrate under force, unfolding of the substrate was detected as an 11 nm extension step. Formation of a mixed disulfide was detected as a 14 nm extension step arising from the cleavage of the 32–75 disulfide in the substrate (unfiltered data shown in light grey).

(E) A mechanical force was applied to a polyprotein consisting of repeated I27^{32–75} domains, in a solution containing reduced PDla.

(F) The substrate was extended, and mixed disulfides were formed between PDla enzymes and a cysteine in each domain, as described in (C). The force was then removed, and the resulting folding and oxidation of the substrate were probed after a preset folding interval Δt_F .

(G) Representative recording showing extension and force measurements for the [*denature* – *folding* – *probe*] force protocol. Arrowheads indicate formation of mixed disulfide complexes with PDla (14 nm steps). After refolding for 5 s, four domains had folded and acquired disulfides, as revealed by the subsequent 11 and 14 nm steps in the *probe* pulse. Other traces revealed refolding without disulfide formation (25 nm step, inset; see also Figure S2B).

(H) Step-size histograms compiled from several recordings confirm that PDla catalyzed oxidative folding in some domains, whereas other domains refolded in a reduced state ($n = 137$).

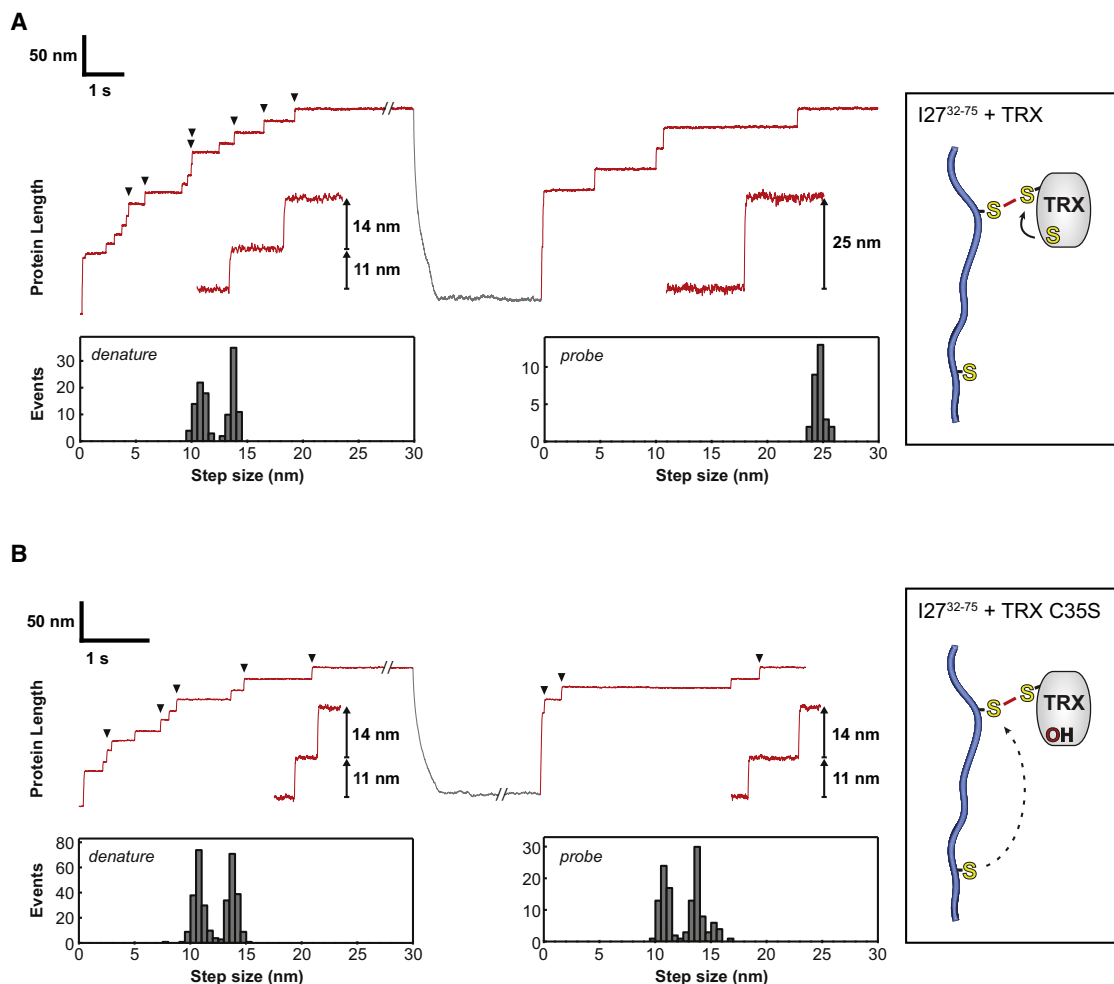


Figure 2. Enzyme Release Determines Outcome of Oxidative Folding

(A) Mixed disulfide complexes with thioredoxin (TRX) do not catalyze disulfide formation in the folding I27^{32–75} polypeptide. In this recording, seven domains were completely extended during the *denature* pulse. Four of these then refolded, albeit without disulfides, as seen from the 25 nm steps in the *probe* pulse. The rapid release mechanism of TRX accounts for its inability to catalyze disulfide formation (right panel) ($n = 61$).

(B) The C35S mutation in TRX replaces a reactive sulfur atom with oxygen and thus prevents spontaneous release of the enzyme (see Figure S3). TRX C35S catalyzed disulfide formation in the folding polypeptide by remaining in the mixed disulfide complex upon substrate folding ($\Delta t_F = 3$ s). Step-size histograms show that disulfides had been formed in all refolded domains ($n = 169$). Arrowheads indicate mixed disulfide complex formation.

Kinetics of Oxidative Protein Folding from an Extended State

A mixed disulfide complex with PDIA enables the catalysis of oxidative folding, yet it is unknown how protein folding is affected by the covalent attachment of this enzyme. Our approach allowed us to directly measure the effect of a covalently bound PDIA on protein folding.

We first set out to establish the refolding properties of I27^{32–75} in isolation, with and without the 32–75 disulfide bond. Using the [*denature* – *folding* – *probe*] protocol, we first measured folding kinetics of the reduced substrate. Figure 4A shows a representative trace for a refolding time $\Delta t_F = 3$ s. Steps of 25 nm are seen in both the *denature* and *probe* pulses, confirming that none of the domains contained disulfide bonds (in the absence of enzymes, we never observed disulfide formation during folding; Figure S5 shows the equivalent experiment with

oxidized I27^{32–75}). A longer refolding time of $\Delta t_F = 10$ s allowed for more domains to refold (Figure 4B). By varying the refolding time Δt_F , we could measure the kinetics of refolding. We found that the reduced protein folded at a rate of 0.27 s^{-1} , whereas presence of the 32–75 disulfide increased the folding rate by nearly 30 times to 7.74 s^{-1} (Figure 4C).

Strikingly, the time course of PDIA-catalyzed oxidative folding was similar to the time course of folding of the reduced substrate (Figure 4C). Despite the steric hindrance caused by covalent attachment, PDIA apparently did not interfere with the folding protein. Single exponential kinetics accounted well for the PDIA-catalyzed oxidative folding data (solid red line in Figure 4C), suggesting a single rate-limiting step late in the oxidative folding pathway. Statistical analysis showed that the rate of oxidation was marginally yet significantly faster than folding ($p < 0.01$), indicating that this rate-limiting step occurred before folding had

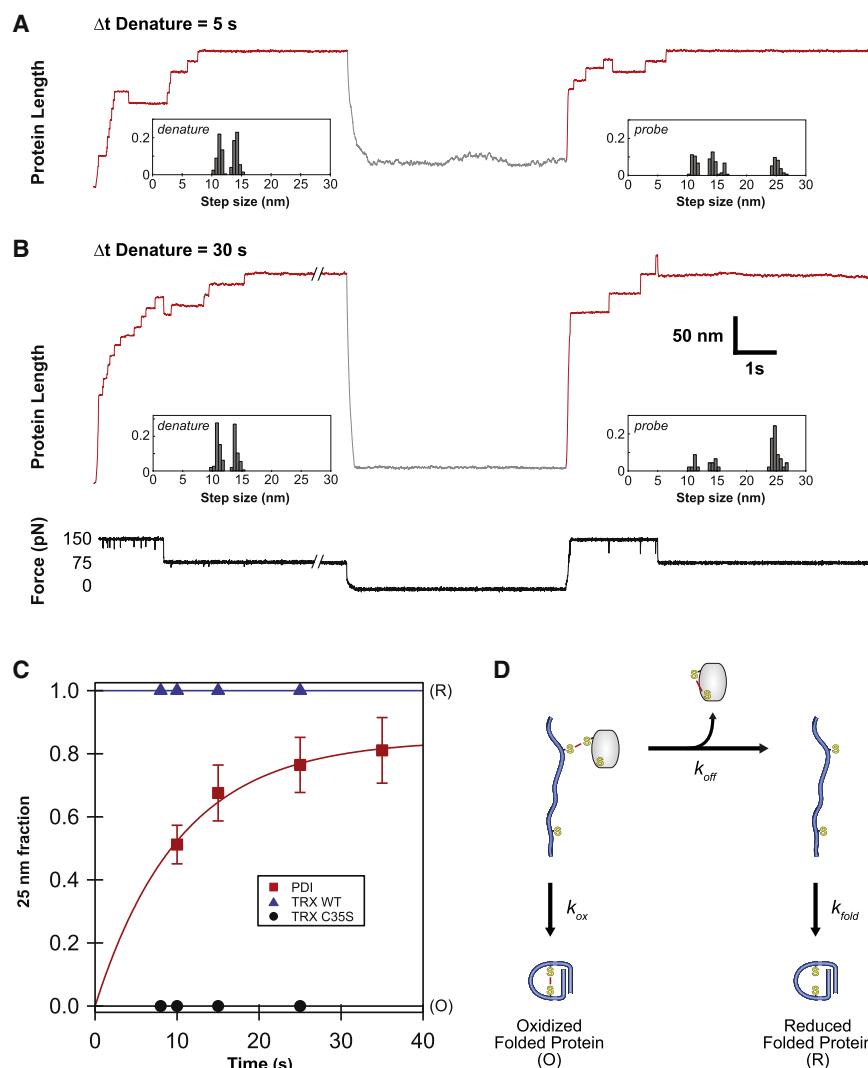


Figure 3. Measurement of PDIa Release Kinetics

(A) In an experiment with a 5 s denature pulse ($\Delta t_D = 5 \text{ s}$), $\sim 50\%$ of PDIa enzymes remained in the mixed disulfide complexes during the subsequent protein-folding interval. As a result, oxidative folding mostly completed successfully, as seen from the predominance of 11 and 14 nm steps in the probe pulse ($n = 105$).

(B) After a 30 s denature pulse ($\Delta t_D = 30 \text{ s}$), $\sim 80\%$ of mixed disulfides had been cleaved through spontaneous release of PDIa. Folding was still observed, but only few of the folded domains contained disulfides, as seen from the predominance of 25 nm steps in the probe pulse ($n = 66$). See also Figure S4A.

(C) Spontaneous enzyme release, measured as the fraction of folded domains that were reduced by the start of the probe pulse (25 nm steps, fraction \pm SEM). The fraction is displayed as a function of total time ($\Delta t_D + \Delta t_F$). The data for PDIa fall between the rapidly releasing TRX and the release-deficient TRX C35S. Assuming the model in (D), the rate of spontaneous PDIa release was calculated from an exponential fit (solid line) ($n > 100$).

(D) Kinetic model including the rate of spontaneous enzyme release (k_{off}), the rate of oxidative folding from the mixed disulfide complex (k_{ox}), and the rate of folding of the reduced substrate (k_{fold}).

dered manner. At a late stage of folding, close in time to the acquisition of the native fold, PDIa catalyzes the formation of an intramolecular disulfide in the substrate. This reaction releases PDIa and allows the substrate to rapidly complete oxidative folding. An earlier study showed exceptionally high reactivity between PDI-substrate mixed disulfides and freely diffusing cysteine-containing peptides

(Darby and Creighton, 1995a). In light of these and our results, it appears that PDI-mediated oxidative folding is rate-limited not by the covalent chemical reaction but rather by the encounter rate of the reacting groups, which in turn is limited by protein folding.

Formation of Interdomain Disulfides Triggers Misfolding

The oxidative folding recordings with I27^{32–75} revealed in the probe pulse sporadic 15 nm steps, which were due to cleavage of interdomain disulfide bonds. Several lines of evidence support this conclusion. The most direct indication came from recordings where the events were clearly separated in time and thus allowed for higher precision when determining the step size. For instance, in the recording shown in Figure 5A, we achieved a spatial resolution better than 0.1 nm by localizing the centroids of Gaussians fitted to 1,000 unfiltered data points before and after each step. This analysis revealed that whereas the step size of the 32–75 reduction events was 13.8 nm (hereafter referred to as 14 nm steps for simplicity), the new steps had

completed. The native state was acquired rapidly after disulfide formation, as inferred from the fast refolding kinetics of the oxidized substrate (Figure 4C). Although PDIa-mediated oxidation could in theory be more accurately described as a multi-exponential process, fitting a double exponential to the PDIa data yielded only marginal improvement of the fit ($\chi^2 = 0.373$ versus $\chi^2 = 0.377$). Curiously, all experiments with enzymes (PDIa and TRX) showed lower absolute values of folding than the experiments without enzymes. However, we observed this effect also in experiments where both the substrate and the enzyme were reduced, wherein no mixed disulfides could have been formed (data not shown). This effect is therefore not caused by mixed disulfide complexes but rather by other, likely noncovalent, enzyme-substrate interactions.

Taken together, our data give an idea of how PDIa catalyzes disulfide formation in the folding protein. PDIa first becomes covalently attached to the substrate by forming a mixed disulfide complex. From there on, the enzyme acts as a passive placeholder, allowing the substrate to collapse and fold in an unin-

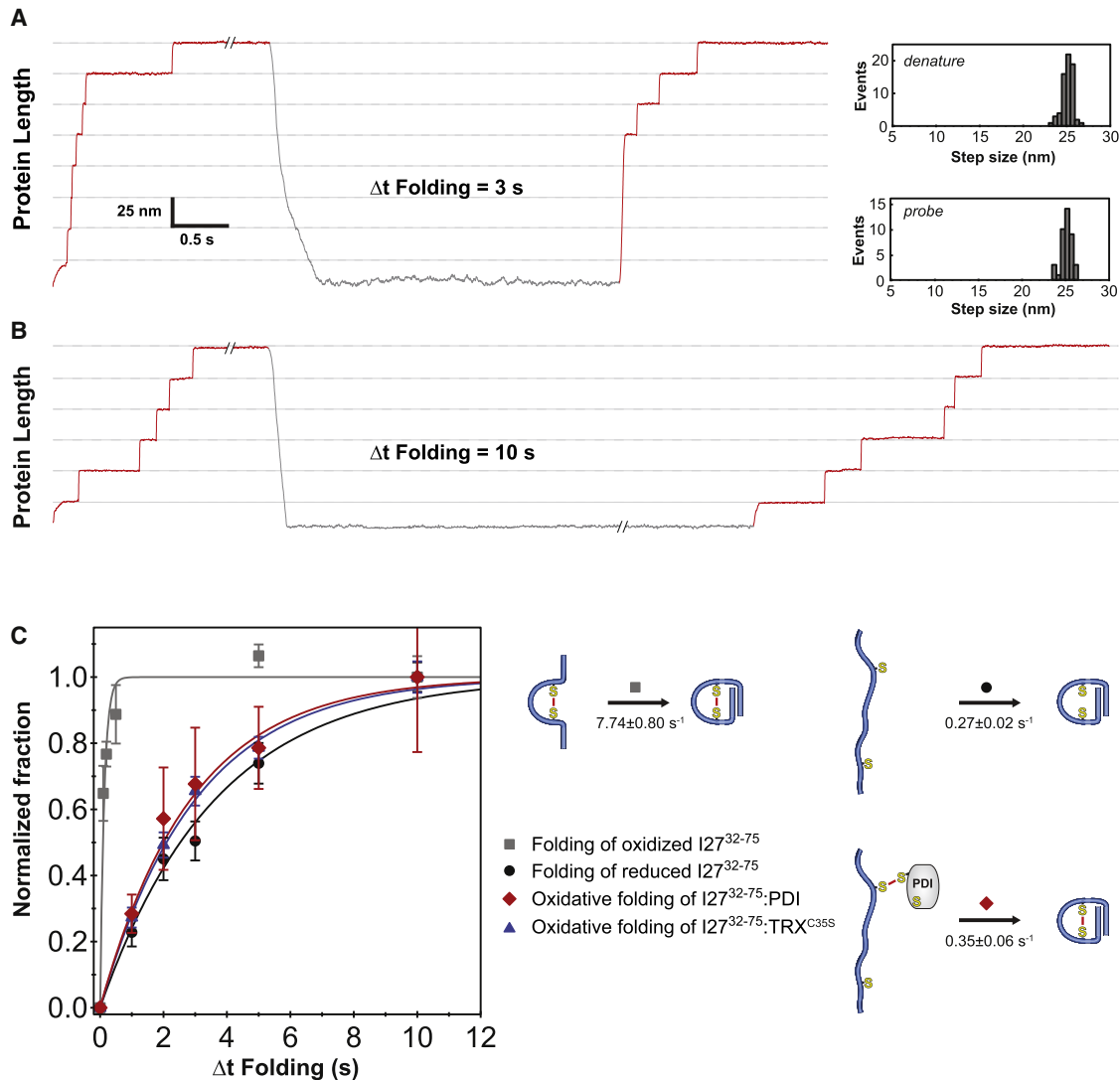


Figure 4. Measurement of Protein Folding from an Extended State

(A) Refolding experiments with prereduced I27³²⁻⁷⁵ polyproteins show no evidence of disulfide formation in the absence of enzymes ($n = 68$).

(B) Longer folding interval (Δt_f) increases refolding probability. Folding kinetics were measured by varying Δt_f .

(C) Time course of folding (gray squares and black circles) and oxidative folding (red diamonds and blue triangles) from an extended state (fraction \pm SEM; $n > 50$). I27 folding is accelerated nearly 30-fold by the presence of the 32–75 disulfide (Figure S5). The rates of disulfide formation catalyzed by PDI and TRX C35S are only marginally faster than the folding rate of the reduced substrate, indicating that disulfide formation occurred late in the oxidative folding process. Errors represent SEM.

a magnitude of 15.4 nm (hereafter referred to as 15 nm steps). The occurrence of 15 nm steps correlated well with the number of initially unfolded domains (Figures S6A and S6B); however, these steps did not represent unfolding events, as they were not induced by a high stretching force. Instead, their step size corresponded exactly to the expected elongation upon cleavage of a disulfide between Cys75 in one I27 domain and Cys32 in the next domain (15.4 ± 0.1 nm measured versus 15.5 nm predicted from Equation S1).

To investigate the prevalence of interdomain disulfides, we compiled an extended histogram from the oxidative folding data with PDI (Figure 5B). We then fit the data with multiple

fixed-width Gaussians and identified three clearly distinct peaks in the *probe* pulse that were not present in the *denature* pulse. One peak was centered at ~ 25 nm and corresponded to the unfolding of reduced domains. The two other peaks were centered at ~ 15 nm and ~ 30 nm and could be assigned to interdomain disulfides (Figure 5E). In total, the interdomain disulfides accounted for $\sim 20\%$ of the data.

Sporadic formation of interdomain disulfides was observed for different substrates (Figure 5D), including I27²⁴⁻⁵⁵ (Figure S7C) and I27 WT (Figure S7B). The high accuracy of our step assignment can be seen in Figure 5E, where the horizontal axis indicates the cysteine separation as a number of residues, and the

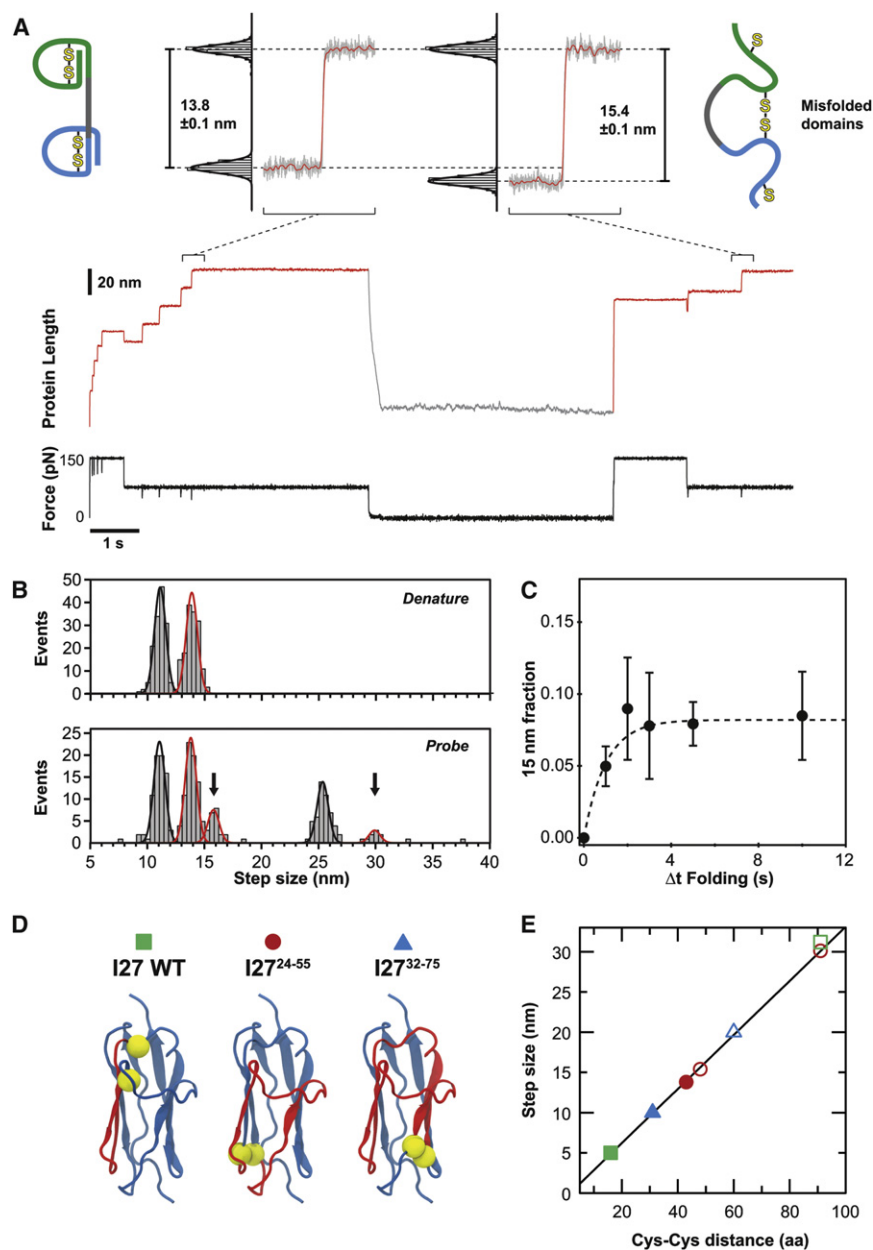


Figure 5. Non-native Interdomain Disulfides Prevent Native Folding

(A) Cleavage of a 32–75 intradomain disulfide resulted in a 13.8 nm step. Interdomain disulfides between Cys75 in one domain and Cys32 in an adjacent domain were detected as 15.4 nm steps. The recording shows unfolding and PDla-mediated disulfide cleavage of four domains in the *denature* pulse. Upon refolding, two interdomain disulfides were formed, but no refolding took place. Cleavage of the interdomain disulfides can be seen in the *probe* pulse as two 15.4 nm steps (values represent mean \pm SEM).

(B) Histograms reveal in the *probe* pulse populations of 15.4 nm and 30 nm steps (black arrows) that appear only after refolding in a mixed disulfide complex with PDla. These anomalous steps were not preceded by corresponding unfolding steps ($n = 302$; solid lines: Gaussian fits with $\sigma = 0.7$ nm).

(C) Kinetics of interdomain disulfide formation by PDla (fraction \pm SEM) ($n > 100$). See also Figure S6.

(D) The three substrates used in this study. Yellow spheres indicate locations of cysteine residues. Red segments are inextensible when an intradomain disulfide is present. Cleavage of a disulfide under force triggers extension of the corresponding red segment (Protein Data Bank [PDB]: 1TIT).

(E) Comparison of observed step sizes (symbols) with predicted values (Equation S1, solid line). Solid symbols represent cleavage of the predominant intradomain disulfides; open symbols represent cleavage of sporadically formed interdomain disulfides.

vertical axis indicates the measured step size. In all our experiments, interdomain disulfides were formed sporadically but did not appear to be favored during PDla-catalyzed oxidative folding.

The I27^{32–75} data showed that formation of interdomain disulfides precluded proper folding. Whereas nearly every 14 nm step in the *denature* and *probe* pulses was accompanied by a corresponding 11 nm step ($N_{11}/N_{14} = 97\% \pm 1\%$ and $91\% \pm 3\%$, respectively), 15 nm steps did not appear to be preceded by corresponding unfolding steps (Figure 5A). An 11 nm step sometimes appeared before a 15 nm step in our recordings. In all of these cases, however, the 11 nm step was also succeeded by a 14 nm step, showing that the 11+14 nm pair corresponded

correctly folded. Formation of non-native interdomain disulfides was thus sufficient to induce protein misfolding.

We explored the possibility that domain swapping had caused the formation of interdomain disulfides. Domain swapping has been observed in I27 in previous studies (Borgia et al., 2011; Oberhauser et al., 1999). However, these studies showed that domain-swapped structures retain mechanical stability. We found no evidence of such structures in our data and therefore conclude that the interdomain disulfides were likely not caused by domain swapping.

Remarkably, the interdomain disulfides appeared at a faster rate than native disulfides (1.0 s^{-1} , Figure 5C). The proportion of interdomain disulfides reached a plateau after ~ 2 s, indicating

to a different domain than the 15 nm step. Furthermore, the appearance of 15 nm steps was negatively correlated with the fraction of domains that successfully refolded (Figure S6A). Domains affected by the interdomain disulfide thus appeared unable to fold into their native conformation. Although the substrate might still attain some degree of structure beyond our detection limit, the absence of mechanical resistance of these structures proves that they are not

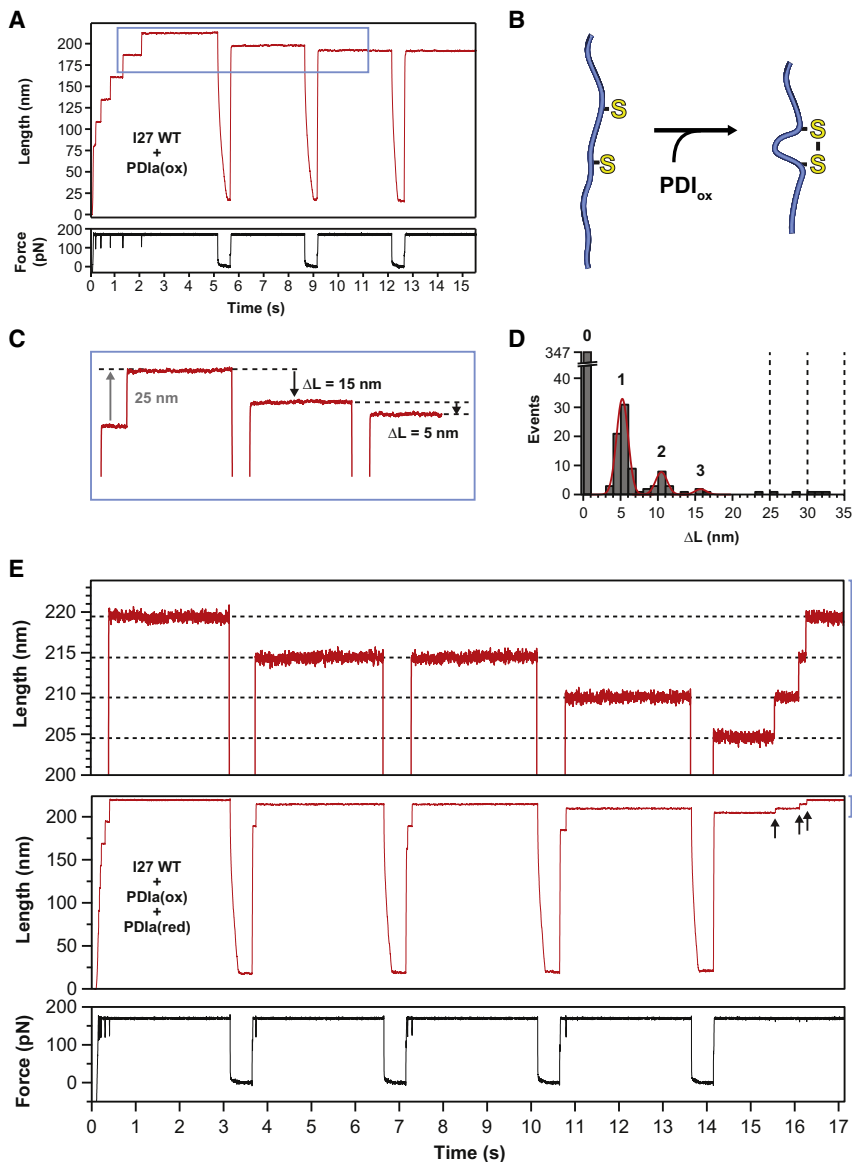


Figure 6. Disulfide Formation Catalyzed by Oxidized PDIA

(A) I27 WT was refolded in solution containing oxidized PDIA. After initial unfolding, the substrate was allowed to collapse for periods of 0.5 s between repeated probe pulses. Formation of a disulfide bond between Cys47 and Cys63 in a domain was detected as a 5 nm shortening of the stretched substrate. Occasionally, multiple oxidation events were detected after a single refolding interval, resulting in 10 or 15 nm steps. (B) PDIA-mediated disulfide formation was detected from the resulting substrate shortening. (C) Magnified view of the recording shown in (A). (D) Histogram of substrate shortenings ΔL in subsequent pulses, compiled from multiple recordings. Numbers above the peaks indicate the corresponding number of intradomain disulfides. Vertical dotted lines indicate predicted shortenings upon formation of interdomain disulfides ($n = 439$). (E) Refolding of I27 WT in solution containing 1:1 molar ratio of reduced PDIA and oxidized PDIA. Similar to the result in (A), disulfide formation was detected as shortening of the substrate. These disulfides could then be cleaved by reduced PDIA enzymes, as seen from the 5 nm extension steps (arrows). See also Figure S7A.

experiments, non-native disulfides could potentially be resolved by reduced PDIA or through intramolecular rearrangement involving the attack of a free cysteine in the substrate, as shown in a previous study (Alegre-Cebollada et al., 2011). However, we did not detect a decrease in interdomain disulfides over time (Figure 5C), indicating that they are relatively stable and not prone to isomerization on the timescale of our experiments.

Formation of Disulfides by Oxidized PDIA

In the ER, PDI-substrate mixed disulfides are thought to form mainly as a result of

that they were formed at an early stage of folding. This is consistent with the substrate being less structured early on during the folding process. If the interdomain disulfides were formed through random collision between cysteines in different domains, then they would be more likely to form at an early stage, as compared to later stages of folding. In this scenario, the folding pathway determines the fidelity of disulfide formation. As domains segregate and tertiary structure starts to form, interdomain contacts lessen, which in turn decreases the probability of forming interdomain disulfides. The accuracy of disulfide formation thus reaches a maximum as the protein approaches the native state.

In cells, non-native interdomain disulfides have been observed during the oxidative folding of low-density lipoprotein receptor (LDL-R) in the ER (Jansens et al., 2002). These disulfides were isomerized into a native configuration on a timescale of hours. In our

oxidized PDI reacting with free cysteines in a substrate (Frand and Kaiser, 1999). To test whether our results were valid also under these conditions, we investigated the reaction of oxidized PDIA with a reduced substrate. Initially, we studied PDIA-mediated oxidation of reduced I27³²⁻⁷⁵. However, we found that folded I27³²⁻⁷⁵ became oxidized at a rate too rapid to enable observation of oxidative folding in a single molecule (Figures S6C and S6D). We therefore chose a substrate with two cysteines that are known to be buried, WT I27 (see Figure 5D). The two cysteines in I27 WT are close in the native structure yet have not been found to form a disulfide (Improta et al., 1996). We speculated that folding in the presence of oxidized PDIA could induce disulfide formation. Formation of an intradomain disulfide in I27 WT shortens its stretched length by 5 nm (Figure 6B). We used a polyprotein consisting of eight repeats of I27 WT to investigate disulfide formation in the presence of

12.5 μM oxidized PDla. The initial staircase in Figure 6A shows only 25 nm steps, verifying that all domains were natively folded and reduced at the beginning of the experiment. When a domain becomes unfolded, oxidized PDla can form mixed disulfide complexes with the newly exposed cysteines. After exposure, followed by a brief refolding interval in the absence of force ($\Delta t_F = 0.5$ s), the substrate was again stretched but did not reach its fully extended length. This shortening, ΔL , may be due to intramolecular disulfide formation (Figures 6B and 6C). A histogram of all observed shortenings for a large number of recordings ($n = 439$) is shown in Figure 6D. Although the majority of refolding intervals did not yield shortenings, three peaks can be seen centered at shortenings of 5, 10, and 15 nm. We reasoned that these three peaks corresponded to the formation of 1, 2, and 3 intradomain disulfide bonds, in separate substrate domains. To prove this hypothesis, we repeated the experiment in the presence of a 1:1 mixture of reduced and oxidized PDla and now observed 5 nm steps as the newly formed disulfides were cleaved by reduced PDla (Figures 6E and S7A). Although present (see Figure S7B), interdomain disulfide formation was not frequently observed in our experiments. We did not observe mechanically stable folded structures in oxidized domains; nevertheless, the data indicate a strong preference for intradomain over interdomain disulfides during PDla-mediated oxidation of I27 WT. As the native fold of the substrate appeared to determine the disulfide formation pattern, this confirms that protein folding drives disulfide formation also in the context of oxidized PDla.

DISCUSSION

For a protein, the path to a native fold is lined with potential traps (Dobson, 2003). Protein folding has become a field of intense research due to its fundamental importance as well as its relevance in numerous diseases. The formation of disulfide bonds adds an additional layer of complexity to the folding pathway of many proteins. For these proteins, cells have evolved dedicated pathways to ensure efficient oxidative folding (Chakravarthi et al., 2009; Sevier and Kaiser, 2002).

In eukaryotes, nascent polypeptides targeted to the ER are exported from the cytosol cotranslationally (Rapoport et al., 1996). Emerging in the ER lumen, polypeptides that contain cysteines form mixed disulfide complexes with oxidase enzymes such as PDI (Bulleid and Freedman, 1988; Molinari and Helenius, 1999). However, it has remained unknown how a mixed disulfide complex affects protein folding and how oxidation and folding are coupled. To investigate this, we used single-molecule AFM to reconstitute mixed disulfide complexes between PDla and an unfolded model protein. Our approach enabled direct and independent measurements of protein folding and disulfide formation.

Does disulfide formation drive protein folding, or conversely, does protein folding provide a driving force for native disulfide formation? Both ideas have been proposed in previous studies (Camacho and Thirumalai, 1995; Wedemeyer et al., 2000; Welker et al., 2001; Wilkinson and Gilbert, 2004), without any consensus being reached in the field. In our experiments, the presence of a mixed disulfide with PDla enabled disulfide formation in a folding protein. Whereas protein folding appeared to rate-limit oxidative

folding, attachment of PDla did not impede the protein-folding rate. Furthermore, native disulfide formation was catalyzed by PDla at a late stage of protein folding. The enzyme remained in the mixed disulfide complex until the substrate had attained a near-native state. At this point, the substrate disulfide was formed, and PDla was released. By enabling oxidation while interfering minimally with protein folding, we conclude that PDla functions more like a passive placeholder than as an active folding catalyst. Our results thus indicate that protein folding provides the driving force during PDla-mediated oxidative folding.

Nascent polypeptides are constrained in an extended state as they traverse the ribosomal exit tunnel and Sec translocase (Becker et al., 2009). Before folding can take place, extended polypeptides first have to undergo entropic and hydrophobic collapse (Berkovich et al., 2010; Fernandez and Li, 2004; Garcia-Manyes et al., 2009). In the absence of force, extended full-length proteins collapse in a fraction of a second and then sample an ensemble of compact conformations that over a time-scale of several seconds acquire their native contacts. Such “molten globule” precursor states have been studied extensively, and they are today recognized as a significant deviation from the classical two-state model of protein folding (Baldwin et al., 2010; Garcia-Manyes et al., 2009; Kuwajima, 1989; Ptit-syn, 1995). We found that the kinetics of disulfide formation corresponded closely to the kinetics of formation of the mechanically stable native state. A molten globule state was thus generally not sufficient for native disulfide formation. Instead, PDla catalyzes disulfide formation with high efficiency only after a large fraction of the native contacts have been acquired (Figure 7).

Cotranslational folding in eukaryotes is limited by the ribosomal translation rate of ~ 5 amino acids per second (Ingolia et al., 2011) (Figure 7). Nuclear magnetic resonance (NMR) studies of cotranslational folding have shown that, although proteins can start acquiring some structural elements while still attached to the ribosome, they acquire their native fold in a domain-wise fashion (Cabrita et al., 2009; Eichmann et al., 2010). For a typical 100 amino acid domain, this leaves around 20 s during which its cysteines are relatively accessible and therefore able to form mixed disulfides with PDI. Based on the estimated concentration of PDI in the ER (up to 1 mM) (Lyles and Gilbert, 1991; Zapun et al., 1992) and the rate of mixed disulfide formation ($>0.1 \text{ mM}^{-1}\text{s}^{-1}$; see Figures S6C and S6D), there is a high probability that a mixed disulfide is present before folding occurs.

When an entire protein domain has been translocated into the ER, the mixed disulfide has to remain in place as the protein folds into its native state. What happens if PDI dissociates before its substrate is completely folded? An exposed substrate cysteine can form a new mixed disulfide. However, protein folding can cause the burial of cysteine residues, which in turn can prevent thiol-disulfide exchange. In an earlier study, prematurely folded domains could acquire disulfides only after spontaneous unfolding, which could take up to an hour (Walker and Gilbert, 1995). To avoid unproductive waiting times and/or consumption of energy through active unfolding of such substrates, PDI needs to introduce disulfides when the nascent protein folds for the first time. This in turn requires the spontaneous off-rate of PDI to be slower than the rate of protein folding. We measured the off-rate of human PDla to be 0.1 s^{-1} . Human PDI is thus an efficient

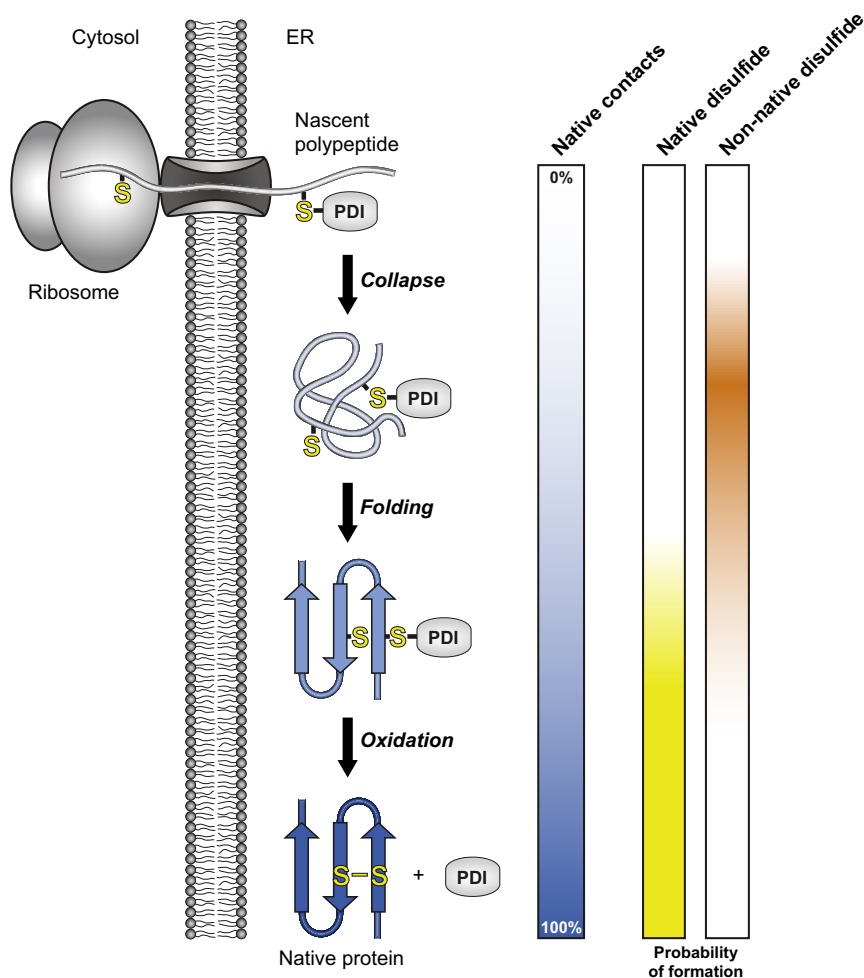


Figure 7. PDI-Mediated Oxidative Folding in the ER

A nascent polypeptide is kept physically extended while emerging from the ribosome and is unable to fold or form disulfide bonds before it enters the ER. PDI enables oxidative folding in the ER lumen by forming a mixed disulfide with a cysteine in the nascent polypeptide. The polypeptide collapses before folding takes place, whereas PDI remains attached throughout this process. Non-native disulfides are sporadically formed during the early stages of folding. PDI favors the formation of native disulfides by allowing the polypeptide to fold into a near-native state before it catalyzes disulfide formation. By allowing protein folding to guide the pairing of cysteines, PDI can catalyze oxidative folding without the need for substrate-specific interactions. Graphs on right side: color intensity indicates percentage of native contacts (blue bar) and probability of disulfide formation (yellow and orange bars).

In view of this, Wilkinson and Gilbert proposed that it is the substrate, rather than PDI, that determines the pairing of cysteines (Wilkinson and Gilbert, 2004). Our data lend strong support to this theory by showing that covalent attachment of PDIa did not significantly interfere with the folding protein. PDIa could thereby favor native disulfides by allowing its substrate to decide, through folding, which cysteines to join. Because this mechanism does not rely on any substrate-specific interactions besides the mixed disulfide, it can explain how a single enzyme can catalyze the oxidative

oxidative folding catalyst for substrates that fold in less than 10 s after they collapse. This time limit is likely sufficient for most secreted proteins and certainly sufficient for small proteins with simple globular structure. However, protein folding can take place on a wide range of timescales. It is therefore tempting to suggest that the off-rate of PDI is adapted to the folding rate of its substrates. The human PDI family has at least 19 members. Perhaps this diversity is required to accommodate the range of protein-folding rates.

Although spontaneous release by PDIa precluded successful oxidative folding in our experiments, this mechanism can serve an important purpose as a release timer in situations where the mixed disulfide complex is unproductive (Walker and Gilbert, 1997).

How does PDI ensure correct pairing of cysteines in proteins with more than one disulfide? For a 4-disulfide protein, there are more than 700 possible disulfide-bonded configurations. Despite the vast number of possibilities, the majority of bonds formed by PDIa in our experiments were the correct intradomain disulfides. In order to catalyze oxidative folding in a wide range of substrates, PDI must rely on a catalytic mechanism that is general yet ensures correct bonding for each specific protein.

folding of a wide variety of proteins. Nevertheless, it is conceivable that other oxidases affect protein folding in diverse ways; for instance, we have found that mixed disulfides with the small molecule glutathione inhibit protein folding (unpublished data).

Oxidative folding in the cell is a highly complex process that involves many components, including oxidoreductases, chaperones, proline *cis-trans* isomerases, and small redox molecules such as glutathione. All of these components can interact with a protein during its folding process, and the resulting complexity has severely hindered detailed mechanistic studies of oxidative folding (Chakravarthi et al., 2009). We have here presented an approach that enables precise control and measurement of both folding and disulfide formation in single protein molecules. These methods can effectively be used to determine differences between oxidase enzymes, as well as the function of other factors involved in oxidative folding in the cell.

EXPERIMENTAL PROCEDURES

Single-Molecule AFM

The details of our custom-made atomic force microscope have been described previously (Fernandez and Li, 2004). We used silicon nitride cantilevers (Bruker MLCT) with a typical spring constant of 15 pN nm⁻¹, calibrated using

the equipartition theorem (Florin et al., 1995). The force-clamp mode provided a feedback time constant of 5 ms. The buffer used in all the experiments was 10 mM HEPES, 150 mM NaCl, 1 mM EDTA, degassed and at pH 7.2. The concentrations used were 10 μ M reduced TRX, 40 μ M reduced TRX C35S, 120 μ M reduced PDI A1, and 12.5 μ M oxidized PDI A1. These enzyme concentrations were chosen so as to yield similar rates of mixed-disulfide formation. The polyprotein substrate was added in a droplet and allowed to bind to a freshly evaporated gold coverslip before the experiments. Every experiment consisted of repeated trials where the tip was pressed against the surface at 1 nN for 0.5 s and subsequently retracted. If attachment was achieved, the pulse protocol was applied until detachment occurred. The oxidative folding force-clamp experiments used a triple-pulse [denature – folding – probe] force protocol. The first pulse was maintained at 130–150 pN for a time long enough to ensure complete unfolding and reduction of the substrate (at least 5 s). The second pulse was set at 0 pN and maintained for the desired amount of refolding time. The third pulse was set at a force identical to the first and maintained until complete unfolding and reduction could be ensured (at least 5 s). For measurement of the data in Figures 3, 4, and 5, split denature and probe pulses were used. This method allowed for a clearer separation of unfolding and reduction steps and has been described earlier (Wiita et al., 2006).

Data Analysis

We used custom-written software in IGOR Pro (Wavemetrics) to collect and analyze data. Recordings were low-pass filtered at 1 kHz for display purposes. Traces were selected based on the fingerprint consisting of at least two unfolding events in the denature pulse. Initially oxidized I27^{32–75} traces exhibiting step sizes other than 11 nm or 14 nm in the denature pulse were excluded from the analysis to ensure homogeneity. For initially reduced substrate samples, 25 nm steps were used as the selection criterion. More than 50% of all traces with repeated steps met these criteria. Only traces showing equal extension at the end of the probe pulse and the end of the denature pulse were included, to ensure that the same protein was stretched in the two pulses. Step-size histograms were generated using all steps >5 nm detected after the initial elastic extension in each force pulse. A 2.5 nm minimum cutoff was applied to the histogram in Figure 6D. Histograms in the main-text figures were compiled from representative experiments. The number of independent observations *n* was counted as the total number of protein domains (as observed in the denature pulse). Standard error of the mean (SEM) for fractions was estimated through the bootstrap method, where each recording was treated as an independent data point. SEM for fit parameters was determined as the standard error for the coefficient in the fit, given the measurement errors of the individual data points.

SUPPLEMENTAL INFORMATION

Supplemental Information includes Extended Experimental Procedures and seven figures and can be found with this article online at <http://dx.doi.org/10.1016/j.cell.2012.09.036>.

ACKNOWLEDGMENTS

This work was supported by grants from the NIH (HL066030 and HL061228 to J.M.F.; CA097061, CA161061, and GM085081 to B.R.S.), HHMI (B.R.S.), the Arnold and Mabel Beckman Foundation (B.R.S.), the Spanish Ministry of Education (A.I.-P.), the Spanish Ministry of Science and Innovation (BIO2009-09562 and CSD2009-00088 to J.M.S.-R.), FEDER (J.M.S.-R.), Fundación Ibercaja (J.A.-C.), and the Training Program in Molecular Biophysics (T32GM008281 to A.K.). P.K. was supported by a Fulbright scholarship. P.K., J.A.-C., and J.M.F. designed the experiments. P.K., J.A.-C., and J.F. performed the experiments and analyzed the data. A.K. and B.R.S. provided PDI A1. A.H. provided TRX. A.I.-P. and J.M.S.-R. provided TRX C35S. P.K., J.A.-C., and J.M.F. wrote the manuscript. We thank the members of the Fernández lab for their illuminating feedback.

Received: January 11, 2012

Revised: July 3, 2012

Accepted: September 5, 2012

Published: November 8, 2012

REFERENCES

- Ainavarapu, S.R., Brujic, J., Huang, H.H., Wiita, A.P., Lu, H., Li, L., Walther, K.A., Carrion-Vazquez, M., Li, H., and Fernandez, J.M. (2007). Contour length and refolding rate of a small protein controlled by engineered disulfide bonds. *Biophys. J.* 92, 225–233.
- Alegre-Cebollada, J., Kosuri, P., Rivas-Pardo, J.A., and Fernández, J.M. (2011). Direct observation of disulfide isomerization in a single protein. *Nat. Chem.* 3, 882–887.
- Baldwin, R.L., Frieden, C., and Rose, G.D. (2010). Dry molten globule intermediates and the mechanism of protein unfolding. *Proteins* 78, 2725–2737.
- Becker, T., Bhushan, S., Jarasch, A., Armache, J.P., Funes, S., Jossinet, F., Gumbart, J., Mielke, T., Berninghausen, O., Schulten, K., et al. (2009). Structure of monomeric yeast and mammalian Sec61 complexes interacting with the translating ribosome. *Science* 326, 1369–1373.
- Berkovich, R., Garcia-Manyes, S., Urbakh, M., Klafter, J., and Fernandez, J.M. (2010). Collapse dynamics of single proteins extended by force. *Biophys. J.* 98, 2692–2701.
- Borgia, M.B., Borgia, A., Best, R.B., Steward, A., Nettels, D., Wunderlich, B., Schuler, B., and Clarke, J. (2011). Single-molecule fluorescence reveals sequence-specific misfolding in multidomain proteins. *Nature* 474, 662–665.
- Bulleid, N.J., and Freedman, R.B. (1988). Defective co-translational formation of disulphide bonds in protein disulphide-isomerase-deficient microsomes. *Nature* 335, 649–651.
- Cabrera, L.D., Hsu, S.T., Launay, H., Dobson, C.M., and Christodoulou, J. (2009). Probing ribosome-nascent chain complexes produced in vivo by NMR spectroscopy. *Proc. Natl. Acad. Sci. USA* 106, 22239–22244.
- Camacho, C.J., and Thirumalai, D. (1995). Modeling the role of disulfide bonds in protein folding: entropic barriers and pathways. *Proteins* 22, 27–40.
- Carvalho, A.P., Fernandes, P.A., and Ramos, M.J. (2006). Similarities and differences in the thioredoxin superfamily. *Prog. Biophys. Mol. Biol.* 91, 229–248.
- Chakravarthi, S., Jessop, C.E., and Bulleid, N.J. (2009). Oxidative folding in the endoplasmic reticulum. In *Oxidative Folding of Peptides and Proteins, Chapter 1.5* (Cambridge, UK: The Royal Society of Chemistry), pp. 81–104.
- Chivers, P.T., and Raines, R.T. (1997). General acid/base catalysis in the active site of *Escherichia coli* thioredoxin. *Biochemistry* 36, 15810–15816.
- Darby, N.J., and Creighton, T.E. (1995a). Characterization of the active site cysteine residues of the thioredoxin-like domains of protein disulfide isomerase. *Biochemistry* 34, 16770–16780.
- Darby, N.J., and Creighton, T.E. (1995b). Functional properties of the individual thioredoxin-like domains of protein disulfide isomerase. *Biochemistry* 34, 11725–11735.
- Debarbieux, L., and Beckwith, J. (2000). On the functional interchangeability, oxidant versus reductant, of members of the thioredoxin superfamily. *J. Bacteriol.* 182, 723–727.
- Di Jeso, B., Park, Y.N., Ulianich, L., Treglia, A.S., Urbanas, M.L., High, S., and Arvan, P. (2005). Mixed-disulfide folding intermediates between thyroglobulin and endoplasmic reticulum resident oxidoreductases ERp57 and protein disulfide isomerase. *Mol. Cell. Biol.* 25, 9793–9805.
- Dobson, C.M. (2003). Protein folding and misfolding. *Nature* 426, 884–890.
- Dong, G., Wearsch, P.A., Peaper, D.R., Cresswell, P., and Reinisch, K.M. (2009). Insights into MHC class I peptide loading from the structure of the tapasin-ERp57 thiol oxidoreductase heterodimer. *Immunity* 30, 21–32.
- Eichmann, C., Preissler, S., Riek, R., and Deuerling, E. (2010). Cotranslational structure acquisition of nascent polypeptides monitored by NMR spectroscopy. *Proc. Natl. Acad. Sci. USA* 107, 9111–9116.
- Fernandez, J.M., and Li, H. (2004). Force-clamp spectroscopy monitors the folding trajectory of a single protein. *Science* 303, 1674–1678.
- Florin, E.L., Rief, M., Lehmann, H., Ludwig, M., Dornmair, C., Moy, V.T., and Gaub, H.E. (1995). Sensing specific molecular-interactions with the atomic-force microscope. *Biosens. Bioelectron.* 10, 895–901.

- Frand, A.R., and Kaiser, C.A. (1999). Ero1p oxidizes protein disulfide isomerase in a pathway for disulfide bond formation in the endoplasmic reticulum. *Mol. Cell* 4, 469–477.
- García-Manyes, S., Dougan, L., Badilla, C.L., Brujic, J., and Fernández, J.M. (2009). Direct observation of an ensemble of stable collapsed states in the mechanical folding of ubiquitin. *Proc. Natl. Acad. Sci. USA* 106, 10534–10539.
- Gething, M.J., and Sambrook, J. (1992). Protein folding in the cell. *Nature* 355, 33–45.
- Gilbert, H.F. (1995). Thiol/disulfide exchange equilibria and disulfide bond stability. *Methods Enzymol.* 251, 8–28.
- Grandbois, M., Beyer, M., Rief, M., Clausen-Schaumann, H., and Gaub, H.E. (1999). How strong is a covalent bond? *Science* 283, 1727–1730.
- Hoffstrom, B.G., Kaplan, A., Letso, R., Schmid, R.S., Turmel, G.J., Lo, D.C., and Stockwell, B.R. (2010). Inhibitors of protein disulfide isomerase suppress apoptosis induced by misfolded proteins. *Nat. Chem. Biol.* 6, 900–906.
- Holmgren, A. (1985). Thioredoxin. *Annu. Rev. Biochem.* 54, 237–271.
- Improta, S., Politou, A.S., and Pastore, A. (1996). Immunoglobulin-like modules from titin I-band: extensible components of muscle elasticity. *Structure* 4, 323–337.
- Ingolia, N.T., Lareau, L.F., and Weissman, J.S. (2011). Ribosome profiling of mouse embryonic stem cells reveals the complexity and dynamics of mammalian proteomes. *Cell* 147, 789–802.
- Jansens, A., van Duijn, E., and Braakman, I. (2002). Coordinated nonvectorial folding in a newly synthesized multidomain protein. *Science* 298, 2401–2403.
- Kadokura, H., and Beckwith, J. (2009). Detecting folding intermediates of a protein as it passes through the bacterial translocation channel. *Cell* 138, 1164–1173.
- Kadokura, H., Tian, H., Zander, T., Bardwell, J.C., and Beckwith, J. (2004). Snapshots of DsbA in action: detection of proteins in the process of oxidative folding. *Science* 303, 534–537.
- Kuwajima, K. (1989). The molten globule state as a clue for understanding the folding and cooperativity of globular-protein structure. *Proteins* 6, 87–103.
- Lappi, A.K., and Ruddock, L.W. (2011). Reexamination of the role of interplay between glutathione and protein disulfide isomerase. *J. Mol. Biol.* 409, 238–249.
- Lundström, J., and Holmgren, A. (1990). Protein disulfide-isomerase is a substrate for thioredoxin reductase and has thioredoxin-like activity. *J. Biol. Chem.* 265, 9114–9120.
- Lundström, J., Krause, G., and Holmgren, A. (1992). A Pro to His mutation in active site of thioredoxin increases its disulfide-isomerase activity 10-fold. New refolding systems for reduced or randomly oxidized ribonuclease. *J. Biol. Chem.* 267, 9047–9052.
- Lyles, M.M., and Gilbert, H.F. (1991). Catalysis of the oxidative folding of ribonuclease A by protein disulfide isomerase: dependence of the rate on the composition of the redox buffer. *Biochemistry* 30, 613–619.
- Martin, J.L. (1995). Thioredoxin—a fold for all reasons. *Structure* 3, 245–250.
- Molinari, M., and Helenius, A. (1999). Glycoproteins form mixed disulphides with oxidoreductases during folding in living cells. *Nature* 402, 90–93.
- Oberhauser, A.F., Marszalek, P.E., Carrion-Vazquez, M., and Fernandez, J.M. (1999). Single protein misfolding events captured by atomic force microscopy. *Nat. Struct. Biol.* 6, 1025–1028.
- Paxson, J.J., Borg, N.A., Horne, J., Thompson, P.E., Chin, Y., Sharma, P., Simpson, J.S., Wielens, J., Piek, S., Kahler, C.M., et al. (2009). The structure of the bacterial oxidoreductase enzyme DsbA in complex with a peptide reveals a basis for substrate specificity in the catalytic cycle of DsbA enzymes. *J. Biol. Chem.* 284, 17835–17845.
- Ptitsyn, O.B. (1995). Molten globule and protein folding. *Adv. Protein Chem.* 47, 83–229.
- Qin, J., Clore, G.M., Kennedy, W.M., Huth, J.R., and Gronenborn, A.M. (1995). Solution structure of human thioredoxin in a mixed disulfide intermediate complex with its target peptide from the transcription factor NF kappa B. *Structure* 3, 289–297.
- Rapoport, T.A., Jungnickel, B., and Kutay, U. (1996). Protein transport across the eukaryotic endoplasmic reticulum and bacterial inner membranes. *Annu. Rev. Biochem.* 65, 271–303.
- Ron, D., and Walter, P. (2007). Signal integration in the endoplasmic reticulum unfolded protein response. *Nat. Rev. Mol. Cell Biol.* 8, 519–529.
- Schröder, M., and Kaufman, R.J. (2005). The mammalian unfolded protein response. *Annu. Rev. Biochem.* 74, 739–789.
- Sevier, C.S., and Kaiser, C.A. (2002). Formation and transfer of disulphide bonds in living cells. *Nat. Rev. Mol. Cell Biol.* 3, 836–847.
- Tu, B.P., Ho-Schleyer, S.C., Travers, K.J., and Weissman, J.S. (2000). Biochemical basis of oxidative protein folding in the endoplasmic reticulum. *Science* 290, 1571–1574.
- Uehara, T., Nakamura, T., Yao, D., Shi, Z.Q., Gu, Z., Ma, Y., Masliah, E., Nomura, Y., and Lipton, S.A. (2006). S-nitrosylated protein-disulphide isomerase links protein misfolding to neurodegeneration. *Nature* 441, 513–517.
- Van den Berg, B., Clemons, W.M., Jr., Collinson, I., Modis, Y., Hartmann, E., Harrison, S.C., and Rapoport, T.A. (2004). X-ray structure of a protein-conducting channel. *Nature* 427, 36–44.
- Walker, K.W., and Gilbert, H.F. (1995). Oxidation of kinetically trapped thiols by protein disulfide isomerase. *Biochemistry* 34, 13642–13650.
- Walker, K.W., and Gilbert, H.F. (1997). Scanning and escape during protein-disulfide isomerase-assisted protein folding. *J. Biol. Chem.* 272, 8845–8848.
- Walker, K.W., Lyles, M.M., and Gilbert, H.F. (1996). Catalysis of oxidative protein folding by mutants of protein disulfide isomerase with a single active-site cysteine. *Biochemistry* 35, 1972–1980.
- Walter, P., Gilmore, R., and Blobel, G. (1984). Protein translocation across the endoplasmic reticulum. *Cell* 38, 5–8.
- Wedemeyer, W.J., Welker, E., Narayan, M., and Scheraga, H.A. (2000). Disulfide bonds and protein folding. *Biochemistry* 39, 4207–4216.
- Welker, E., Wedemeyer, W.J., Narayan, M., and Scheraga, H.A. (2001). Coupling of conformational folding and disulfide-bond reactions in oxidative folding of proteins. *Biochemistry* 40, 9059–9064.
- Wiita, A.P., Ainavaram, S.R., Huang, H.H., and Fernandez, J.M. (2006). Force-dependent chemical kinetics of disulfide bond reduction observed with single-molecule techniques. *Proc. Natl. Acad. Sci. USA* 103, 7222–7227.
- Wiita, A.P., Perez-Jimenez, R., Walther, K.A., Gräter, F., Berne, B.J., Holmgren, A., Sanchez-Ruiz, J.M., and Fernandez, J.M. (2007). Probing the chemistry of thioredoxin catalysis with force. *Nature* 450, 124–127.
- Wilkinson, B., and Gilbert, H.F. (2004). Protein disulfide isomerase. *Biochim. Biophys. Acta* 1699, 35–44.
- Zapun, A., Creighton, T.E., Rowling, P.J., and Freedman, R.B. (1992). Folding in vitro of bovine pancreatic trypsin inhibitor in the presence of proteins of the endoplasmic reticulum. *Proteins* 14, 10–15.